Journal of the Serbian Chemical Society
JSCS-info@shd.org.rs • www.shd.org.rs/JSCS

J. Serb. Chem. Soc. 90 (11) 1303–1315 (2025)
JSCS–5455

Original scientific paper
Published 13 November 2025

A novel Zn(II) coordination compound exhibits selective and sensitive detection of Fe^{3+} and acetylacetone

RUI DAI[1,2], YUETONG WANG[1], HUA ZHANG[1] and ZHIGUO KONG[1,2]*

[1]*Department of Chemistry, Jilin Normal University, Siping 136000, China and* [2]*Key Laboratory of Preparation and Applications of Environmental Friendly Materials, Jilin Normal University, Ministry of Education, Changchun 130103, China*

(Received 2 June, revised 1 July, accepted 15 September 2025)

Abstract: Pyridine derivatives have strong coordination ability, tunable electronic, optical properties and excellent stability as ligands. Their substituent engineering and conjugation extension provides an ideal platform for the construction of efficient fluorescent probes, catalysts and biological functional materials. Based on this, a new coordination compound $[Zn(phen)(L)(H_2O)]\cdot 4H_2O$ was synthesized under solvothermal conditions used 1,10-phenanthroline (phen), 3-carboxy-1-carboxymethyl-2-oxidopyridinium (H_2L) and Zn(II). The crystal structure and composition of the coordination compound were confirmed by single crystal X-ray diffraction and thermogravimetric analysis. Structural analysis confirmed by single crystal X-ray diffraction reveals its unique coordination geometry. In addition, it exhibits significant luminescence, making it a candidate for sensing applications. The luminescence and sensing properties of the coordination compound were investigated in detail. The K_{sv} values for the detection of Fe^{3+} and acac were found to be 3.29×10^5 and 6.67×10^5 M^{-1}, which confirmed high and efficient sensing ability of the synthesized sensor.

Keywords: zinc(II); coordination compound; solvothermal reaction; X-ray crystallography; fluorescence sensing.

INTRODUCTION

Acetylacetone (acac) is an organic coordination compound belonging to the *β*-diketone class, known for its excellent coordination ability and volatility. It is widely used in metal organic synthesis, catalyst preparation, and drug chemistry. However, its safety issues during actual use are increasingly receiving attention.[1] Studies show that acute exposure to acetylacetone through respiratory or skin contact can cause significant harm to the human body: its vapor has irritant effects on mucous membranes and respiratory tracts, and long-term exposure may lead to

* Corresponding author. E-mail: kongzhiguo2007@163.com
https://doi.org/10.2298/JSC250602069D

liver and kidney dysfunction.[2] Additionally, the environmental persistence of this substance should not be overlooked, its hydrophilicity also makes it easy to diffuse with water flow, pollute groundwater sources, destroy the integrity of aquatic biological cell membranes, inhibit algae photosynthesis and cause fish gill tissue damage.[3]

In addition, as an important representative of transition metal ions, Fe^{3+} has multiple functions in nature and industry, covering biological metabolism, catalytic reaction and environmental remediation.[4,5] However, ecological studies have shown that Fe^{3+} has significant toxicity to aquatic organisms.[6] Under occupational exposure scenarios, long-term inhalation of Fe^{3+} containing dust may cause pulmonary fibrosis, and the high solubility of Fe^{3+} in acidic environment will further enhance its bioavailability.[7] Besides, Fe^{3+} easily forms complexes with organic matter such as humic acid in soil and can enhance migration ability, destroy microbial community balance and threaten ecosystem stability.[8] In addition, excess iron ions in the body may cause various hazards, such as kidney failure, neurological disorders and certain types of cancer. Excessive iron can also cause health risks such as organ damage, increased risk of infection and digestive problems. Therefore, it is necessary to find a quick and efficient method for detecting Fe^{3+}, which has attracted increasing attention in environmental and medical fields.[9]

As a transition metal, Zn(II) is particularly suitable for the preparation of photoluminescent complexes because of their zero crystal field stability and their unique d^{10} configuration, which makes them absent from the potential quenching process caused by the d–d transition.[10–12] Zn is an essential trace element for human body, its complex easily metabolize under physiological conditions[13] and its cytotoxicity is significantly lower than that of heavy metal complexes (such as Cd^{2+} and Hg^{2+}).[14,15] Zn-based MOF fluorescent probes are gaining popularity for their high sensitivity, selectivity and stability.[16,17]

In this paper, a coordination compound $[Zn(phen)(L)(H_2O)]\cdot 4H_2O$ was synthesized by solvothermal reaction using transition metal Zn (II), 1,10-phenanthroline (phen) and 3-carboxy-1-carboxymethyl-2-oxidopyridinium (H_2L) as raw materials. Detailed studies on its luminescent and sensing performance have found that it has good luminescent sensing performance for Fe^{3+} and acac which gives it significant application potential, such as the detection of Fe^{3+} and acac in water samples, the detection of Fe^{3+} in drugs, the detection of acac residue in chemical plants, *etc*.

EXPERIMENTAL

Materials and methods

All chemicals used for syntheses and characterization were reagent-grade and used as received from commercial sources, without further purification. PXRD were carried out on a Bruker – AXS Smart CCD X-ray diffractometer. Fluorescence experiments were carried out on

the RF-6000 fluorescence spectrophotometer. Thermogravimetric analysis (TGA) was performed on a NETZSCH STA 449F3 thermal analyzer.

Synthesis of [Zn(phen)(L)(H_2O)]·4H_2O

A mixture of $ZnSO_4$ (0.0288 g, 0.1 mmol), H_2L (0.0112 g, 0.06 mmol), phen (0.0186 g, 0.1 mmol), H_2O (2.5 ml) and DMF (2.5 ml) were sealed in a glass vial. After heating to 88 °C and maintaining the temperature for 72 h, heating was stopped to obtain colorless transparent rectangular-shaped crystals after cooling at a rate of 5° C per hour. Yield: 0.0221 g (41 %) based on Zn. Anal. (%); Calcd. for $C_{20}H_{23}N_3O_{10}Zn$: C, 45.26; H, 4.37; N, 7.92; Found %: C, 44.80; H, 4.32; N, 7.82.

X-ray crystallography

At 298(2)K, a Rigaku Raxis-Rapid diffractometer equipped with a graphite monochromator (MoKα radiation, λ = 0.71073 Å) was used to X-ray diffractometer analyze the single crystal, SIR2014 was used to solve the structure by direct method, and SHELXL2018/3 was used to optimize the F^2 by the full matrix least squares method.

A crystal of suitable size was selected by using an optical microscope, and the crystal size was determined to be 0.232 mm×0.211 mm×0.191 mm, and single crystal diffraction data were collected at a temperature environment around 25 ℃. References were analyzed and refined.[18,19] Hydrogen atoms participate in final structure refinement (N–H, 0.86 Å, C–H, 0.93 Å), *Uiso*(H) = 1.2 Ueq. The final R = 0.0477, wR = 0.1162. (w = 1/[$s2$(*Fo2*) + (0.0568P)2 + 0.7642P], P = (*Fo2* + 2*Fc2*)/3), S = 1.045. The crystallographic summary of [Zn(phen)(L)(H_2O)]·4H_2O (1) is shown in Table I, bond lengths and bond angles in Table II and hydrogen bonds in Table III.

TABLE I. Crystal data, data collection and refinement details

Chemical formula	$C_{20}H_{23}N_3O_{10}Zn$
Formula weight	530.78
Temperature	298(2) K
Wavelength	0.71073 Å
Crystal system	triclinic
Space group	$P\bar{1}$
a / Å	9.134(3)
b / Å	10.539(4)
c / Å	12.228(4)
α / °	77.003(6)
β / °	77.770(6)
γ / °	85.245(6)
V / Å^3	1120.2(7)
Z	2
Density (calculated)	1.574 mg/m^3
F(000)	548
Final R indices (I > 2$sigma$(I))	$R1$ = 0.0477, $wR2$ = 0.1162
S	1.045
Absorption coefficient	1.158 mm^{-1}
Crystal size	0.232 mm×0.211 mm×0.191 mm
Absorption correction	Semi-empirical from14 ≤ l ≤ 14
Max. and min. transmission	0.809 and 0.775

TABLE I. Continued

Index ranges	$-10 \le h \le 9$, $-12 \le k \le 9$, $14 \le l \le 14$
Independent reflections	3847 (R(int) = 0.0263)
Reflections collected	5718
Refinement method	Full-matrix least-squares on F^2
Data/restraints/parameters	3847 / 0 / 307
Goodness-of-fit on F^2	1.003
Final R indices ($I > 2sigma(I)$)	$R1$ = 0.0477, $wR2$ = 0.1162
Final R indexes (all data)	$R1$ = 0.0606, w$R2$ = 0.1281
$\Delta\rho_{max}$, $\Delta\rho_{min}$, e Å^{-3}	0.512 / –0.505
Flack parameter	n/a

The crystallographic data were deposited with the Cambridge Crystallographic Data Centre (CCDC no. 2453636). Copies of this information can be obtained free of charge at: www.ccdc.cam.ac.uk or from the CCDC, 12 union Road, Cambridge CB2 1EZ, UK (fax: 0044 1223 336 033; e-mail: deposit@ccdc.cam.ac.uk).

TABLE II. Selected bond lengths and bond angles

Bond	Distance, Å	Bond	Distance, Å
N(2)–Zn(1)	2.117(3)	O(3)–Zn(1)	2.044(2)
N(3)–Zn(1)	2.092(3)	O(4)–Zn(1)	1.981(3)
O(1W)–Zn(1)	2.005(3)		
Bonds	Angle, °	Bonds	Angle, °
O(4)–Zn(1)–O(3)	87.46(10)	O(4)–Zn(1)–N(2)	87.62(12)
O(1W)–Zn(1)–O(3)	104.26(11)	O(1W)–Zn(1)–N(2)	104.33(11)
O(4)–Zn(1)–N(3)	154.63(13)	O(3)–Zn(1)–N(2)	151.35(11)
O(1W)–Zn(1)–N(3)	100.64(11)	N(3)–Zn(1)–N(2)	79.49(13)
O(3)–Zn(1)–N(3)	93.44(11)		

TABLE III. Geometrical parameters for intermolecular interactions; symmetry transformations used to generate equivalent atoms: ^{i}–x+1, –y, –z+1; ^{ii}x, y–1, z; ^{iii}–x+1, –y, –z; ^{iv}–x, –y+1, –z+1; ^{v}–x+1, –y+1, –z+1; ^{vi}x, y+1, z+1; ^{vii}x, y+1, z

D–H···A	d(D–H) / Å	d(H···A) / Å	d(D···A) / Å	∠DHA, °
O(1W)–H(1A)···O(5W)^{ii}	0.85	1.77	2.567(4)	156.6
O(1W)–H(1B)···O(5)^{iii}	0.85	1.80	2.640(4)	169.2
O(2W)–H(2A)···O(2)	0.85	2.01	2.798(5)	154.0
O(2W)H(2B)···O(2W)^{iv}	0.85	2.24	2.813(7)	124.7
O(3W)–H(3A)···O(4W)^{v}	0.85	1.94	2.759(5)	162.7
O(4W)–H(4A)···O(1)^{i}	0.86	2.10	2.891(4)	152.6
O(4W)–H(4B)···O(5)^{vi}	0.85	2.11	2.858(4)	147.8
O(5W)–H(5A)···O(2)^{iv}	0.85	1.88	2.705(4)	162.4
O(5W)–H(5B)···O(1)^{vii}	0.86	2.13	2.760(4)	129.7

Fluorescence sensing experiments

The following procedure was carried out: 3 mg of the coordination compound was dissolved in 9 mL of water, subjected to ultrasonic treatment, and then allowed to stand at room temperature for three days. The supernatant was then collected for fluorescence testing.[20]

RESULTS AND DISCUSSION

Crystal structure description

Single crystal X-ray diffraction structure analysis indicates that the coordination compound belongs to the triclinic crystal system with the space group $P\bar{1}$: the key the structure data are presented in Table I. The asymmetric unit is composed of a crystallographically independent Zn^{2+}, one L ligand, one phen ligand, one coordination water molecule and four free water molecules. The Zn^{2+} in complex is five-coordinated. The Zn^{2+} is attached to two oxygen atoms (O3, O4), two nitrogen atoms (N2, N3), and one coordinated water molecule (O1) from three different ligands (Fig. 1) in a twisted triangular bipyramid configuration. The geometry of the coordination environment is nearly regular square-pyramidal, with a geometric distortion index of $\tau_5 = 0.05$.

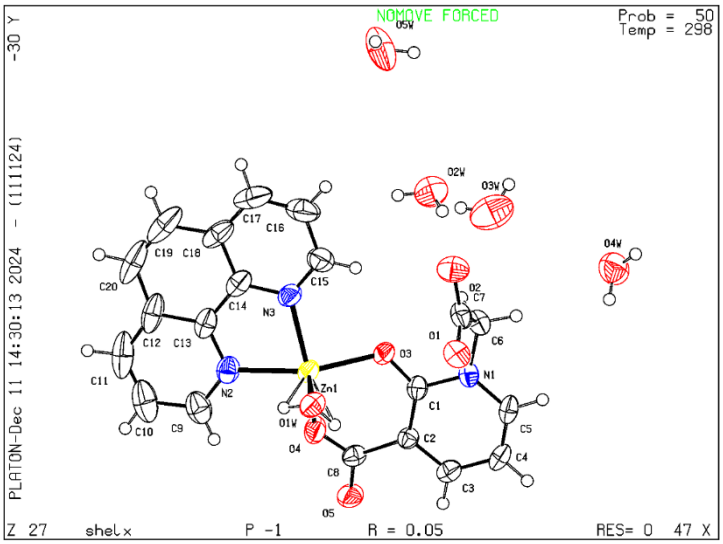

Fig. 1. Coordination environment of Zn^{2+} in the coordination compound. Displacement ellipsoids are drawn at the 50 % probability level and H atoms have been omitted for clarity.

The 1D chain is formed by the π–π interaction (Fig. 2a) between the pyridine ring (N1,C1) and the phenanthroline ring ($N(2)^{viii}/N(3)^{viii}/C(9)^{viii}$–$C(20)^{viii}$ (symmetry codes: $^{viii}x+1, y, z$)) of the adjacent unit. The shortest distances from the centroid to the centroid and from the centroid to the plane of the two rings are 3.693(2) and 3.4238(15) Å, respectively, and the dihedral angle between the two planes is 6.56(15)°. The 1D chain structure connects another adjacent 1D chain structure by hydrogen bonds (Table III) to form 1D double chains (Fig. 2b).[21] Eventually, the 1D double chains structure stacks up into a 3D network structure *via* hydrogen bonds (Fig. 3).[22]

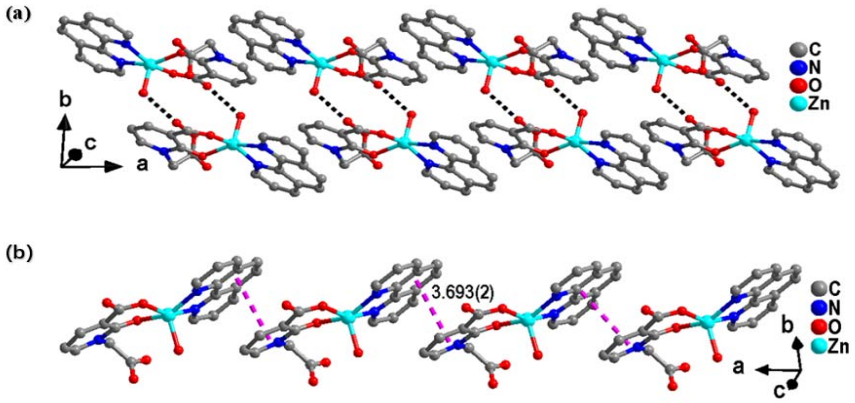

Fig. 2. a) 1D chain structure is formed by π–π interaction. b) 1D double chain structure formed by hydrogen bonding.

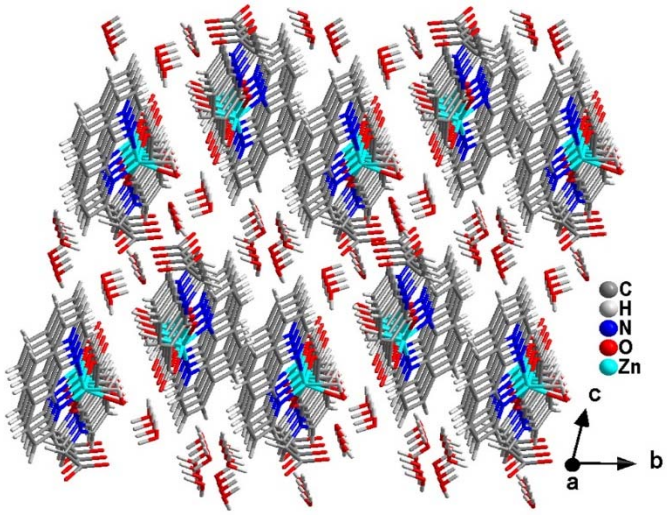

Fig.3.The 3D network structure.

PXRD analyses

In order to test the phase purity of the coordination compound, the powder X-ray diffraction analysis was carried out using Bruker-AXS Smart CCD X-ray diffractometer. The experimental result (Fig. 4) shows that the experimental peak value of the coordination compound is consistent with the one simulated by single crystal X-ray diffraction, which indicates that the good phase purity of the coordination compound, a certain degree of preferred orientation of crystallites is observed, as evidenced by the increase in intensity of discrete peaks with rising 2θ values.

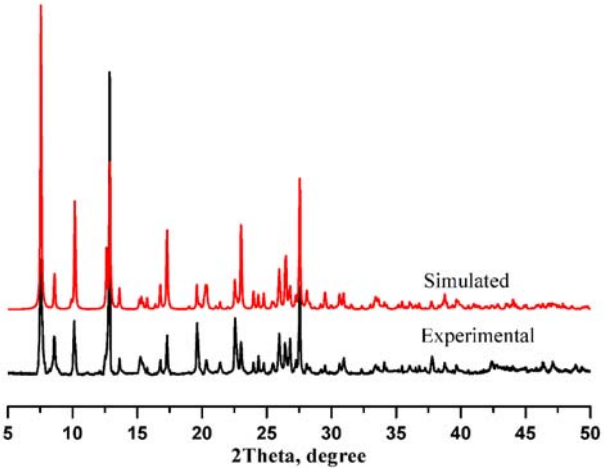

Fig. 4. PXRD patterns of the coordination compound.

TGA analysis of the coordination compound

Analysis shows (Fig. 5) that there is a slight increase in the coordination compound weight near 50°, which can be attributed to carbon dioxide and water molecules in the air. When the temperature rises to 150°, the weight of the coordination compound decreases by about 3.4 %. This is because the departure of unstable coordinated water molecules in the complex molecular framework, followed by a relatively gradual decrease of about 10 % in the coordination compound weight until the temperature rises to 270°, which is due to evaporation of four free water molecules within the complex molecular framework. The result is higher than actual, possibly due to incomplete drying of the sample, followed by a sharp decrease in the coordination compound weight immediately before the temperature rises to 420°. This remarkable decrease is related to the thermal decomposition of phen ligand and organic group $C_8H_5NO_5$ of L. At 453°, the ligand has not completely decomposed, and the weight of the coordination compound continues to decrease at a relatively smooth rate after heating, but the decomposition rate is slower. The above TGA results show that the coordination compound is unstable when heated, the whole framework is gradually collapsing and the results are basically consistent with the crystal structure.[24]

Photoluminescence properties

The fluorescence spectra of phen, H_2L and the coordination compound were investigated in the solid state (Fig. 6a). As shown, the coordination compound in solid state displays good emission characteristics at 366 nm (λ_{ex} = 250 nm), whereas ligands show emission with fluorescence peaks at 363 and 380 nm for phen (λ_{ex} = 280 nm) and 387 nm for H_2L (λ_{ex} = 325 nm). It is obvious that the

peak positions of the coordination compound and phen are very close. Which is attributed not only to the coordination between metal centers and ligands, but also to the superposition of the two luminous peaks of the phen ligand.

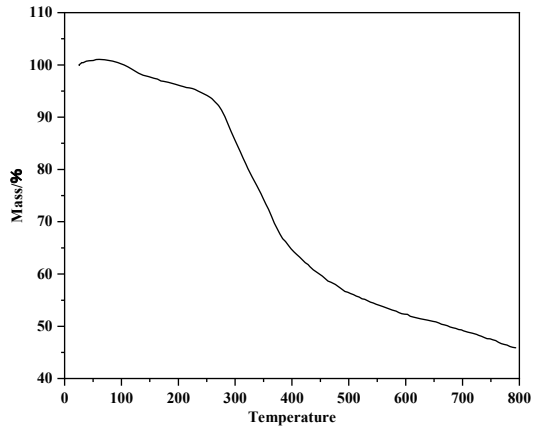

Fig. 5. The TGA of the coordination compound.

The liquid fluorescence of the coordination compound was also examined (Fig. 6b). When prepared as a 3mg/9ml solution, it has a sharp excitation peak at 363nm. Therefore, it can be seen that water has almost no effect on its luminescence, so water was chosen as the solvent for subsequent tests.

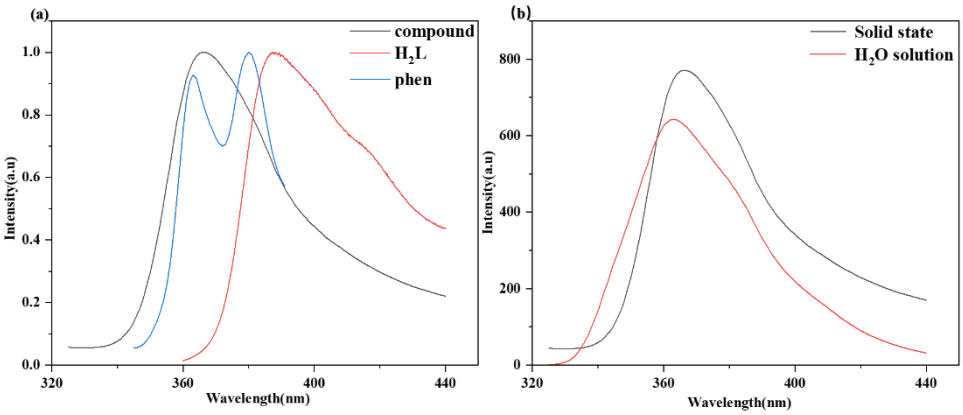

Fig. 6. a) Solid-state emission spectra of the coordination compound, phen and H_2L. λ_{ex}: 250 nm for the coordination compound, 248 nm for phen, and 325 nm for H_2L; b) the emission spectra of the coordination compound in solid state and H_2O solution. λ_{ex}: 250 nm for the coordination compound.

Fluorescence detection of the coordination compound for different cations

14 different metal chloride salts $M(Cl)_x$ (M=Mg^{2+}, Ba^{2+}, Ca^{2+}, Cd^{2+}, K^+, Ni^{2+}, Zn^{2+}, Cr^{3+}, Co^{2+}, Mn^{2+}, Nd^{3+}, Cu^{2+}, Na^+ and Fe^{3+}) with a concentration of

0.01 mol/L were prepared and used for fluorescence sensing testing. The results showed that the addition of different cationic solutions had different effects on the fluorescence intensity of the coordination compound. In particular, the addition of Fe^{3+} significantly reduced the fluorescence intensity of coordination compound (Fig. 7a). To reveal the effect of Fe^{3+} concentration on the fluorescence intensity of the coordination compound composites, the concentration--dependent change in the luminescence intensity of the coordination compound in solution was detected. As shown in Fig. 7b, with the increase of Fe^{3+} concentration from 0 to 3.8×10^{-4} M, the quenching effect of fluorescence in the suspension can be clearly observed. When the concentration of Fe^{3+} is 3.8×10^{-4} M, the luminescence of the suspension is almost completely quenched, and this phenomenon can be easily observed with the naked eye under a portable ultraviolet lamp (excitation wavelength of 254 nm) (Fig. 7b, inset). The linear relationship is good in the range of 2.5×10^{-5} to 3.8×10^{-4} M, with an R^2 value of 0.98634 (Fig. 7c). In addition, the selectivity of coordination compound for Fe^{3+} is performed by an anti-interference experiment, showing that the presence of other cations does not affect the detection of Fe^{3+} (Fig. 7d). According to the Stern–Volmer equation: $(I_0/I)-1 = K_{sv}[C]$ (I_0 represents the initial fluorescence intensity of the coordination compound without the addition of Fe^{3+}, I represents the fluorescence intensity of the coordination compound after the addition of Fe^{3+}, [C] represents the concentration of Fe^{3+} solution and K_{sv} is the fluorescence quenching constant M^{-1}). *LOD* is determined by the formula $LOD = 3\sigma/K_{sv}$, (σ is the relative standard deviation of the blank solution). Finally, luminescent titration demonstrates the *LOD* of 5.25×10^{-5} M for Fe^{3+}.

Fluorescence detection of the coordination compound for different organic reagents

Based on the excellent luminescent properties of the coordination compound, fluorescence spectroscopic studies were conducted on eight organic reagents including methanol (MeOH), ethanol (EtOH), acetonitrile (MeAN), isopropanol (IPA), acetone (ACE), *N*,*N*-dimethylformamide (DMF), *N*,*N*-dimethylacetamide (DMA) and acetylacetone (acac). The results showed that the fluorescence intensity of the coordination compound decreased significantly with the addition of various organic reagents, especially acac (Fig. 8a). To further explore the relationship between the concentration of acac and the fluorescence intensity of the coordination compound, a quantitative experiment was performed. The fluorescence quenching effect of the suspension can be clearly observed with the acac concentration increases from 0 to 8.2×10^{-4} M. When the concentration of acac is 2.5 μM, the luminescence of the suspension almost completely disappears (Fig. 8b). The linear relationship is good in the range of 0.15 to 0.51 mM, with an R^2 value of 0.99837 (Fig. 8c). In addition, the selectivity of the coordination com-

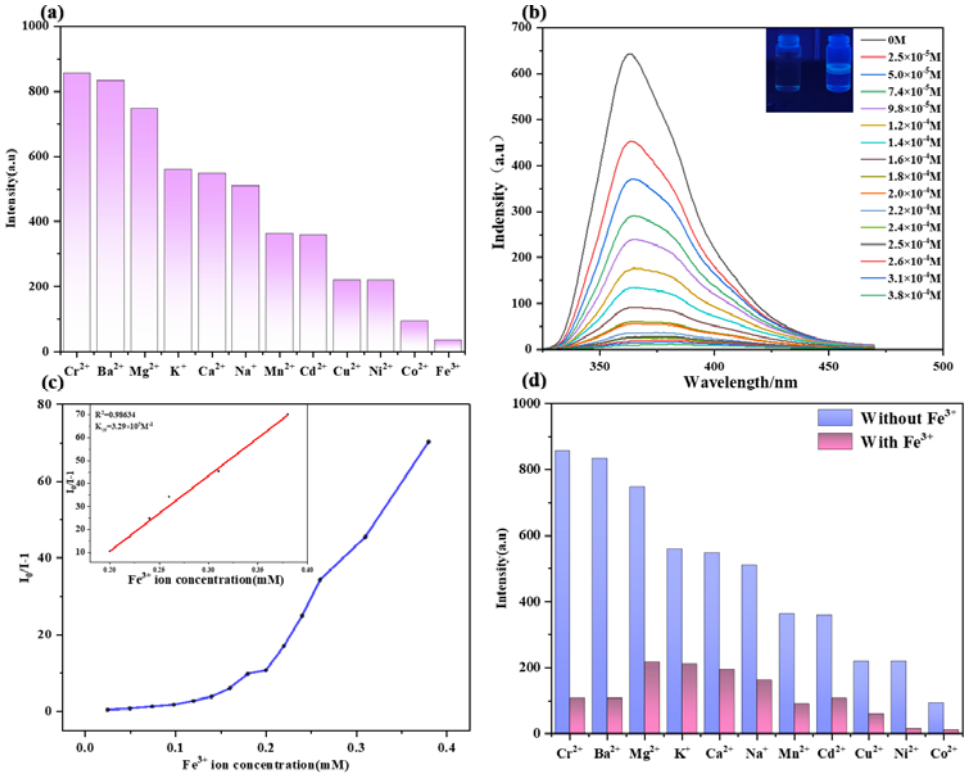

Fig. 7. a) The influence of fluorescence intensity of the coordination compound in the presence of various cationic solutions; b) fluorescence spectra of the coordination compound in aqueous solution with different concentrations of Fe^{3+}; c) fluorescence Stern–Volmer (S–V) equation and the linear relationship of (I_0/I)–1 with Fe^{3+} concentration; d) competitive experiments of the coordination compound in sensing Fe^{3+} with the interference of other metal ions.

pound for acac is performed by an anti-interference experiment, showing that the presence of other cations does not affect the detection of acac (Fig. 8d). Finally, to further evaluate the effect of luminescent titration, the *LOD* was calculated to be 3.4×10^{-5} M by formula $3\sigma/K_{SV}$, verifying the sensitivity of the coordination compound to the detection of acac.

CONCLUSION

In this paper, a new coordination compound was synthesized successfully by solvothermal reaction with Zn^{2+}, 1,10-phenanthroline and 3-carboxy-1-carboxymethyl-2-oxidopyridinium as raw materials and characterized by single crystal X-ray diffraction, TG and PXRD. Single crystal X-ray diffraction shows that the coordination compound further forms 1D by π–π interactions, then 1D layered structure is formed through hydrogen bonds, and 3D supramolecular structure is further accumulated. The experimental results of powder XRD show that the lig-

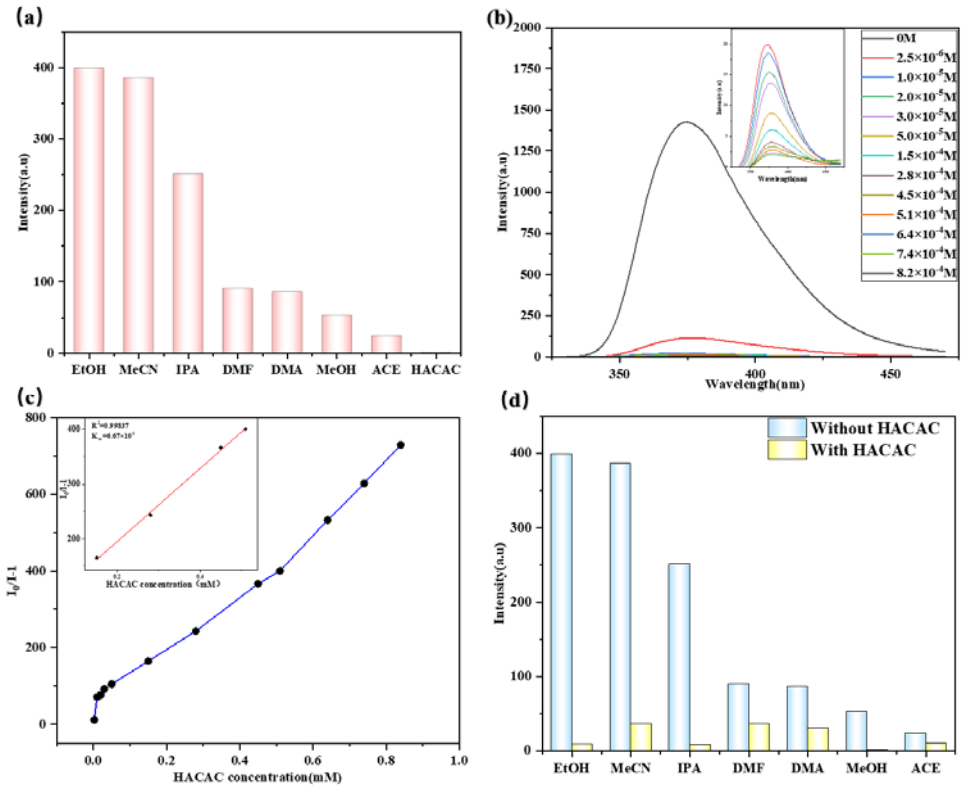

Fig. 8. a) The influence of fluorescence intensity of the coordination compound in the presence of various organic reagents; b) fluorescence spectra of the coordination compound in aqueous solution with different concentrations of acac; c) fluorescence Stern–Volmer (S–V) equation and the linear relationship of $(I_0/I)–1$ with acac concentration; d) comparison of the luminescence intensity of the coordination compound in the presence of acac- mixed organic reagents.

and has been successfully coordinated. The thermogravimetric test results show that it has thermal stability at a certain temperature.

The results of fluorescence sensing experiments show that the coordination compound have good luminescence sensing properties for Fe^{3+} and acac, with minimum *LOD* values of 5.25×10^{-5} M and 3.4×10^{-5} M. Further research will include the luminescence mechanism and practical applications, and it is expected that will have better prospects for use in the future.

Acknowledgements. The authors are grateful to the Scientific and Technological Developing Project of Jilin Province (No. YDZJ202501ZYTS454) for some of the syntheses carried out.

ИЗВОД

НОВИ ЦИНК(II) КОМПЛЕКС ЗА СЕЛЕКТИВНУ И ОСЕТЉИВУ ДЕТЕКЦИЈУ Fe^{3+} И АЦЕТИЛАЦЕТОНА

RUI DAI[1,2], YUETONG WANG[1], HUA ZHANG[1] и ZHIGUO KONG[1,2]

[1]Department of Chemistry, Jilin Normal University, Siping 136000, China и [2]Key Laboratory of Preparation and Applications of Environmental Friendly Materials, Jilin Normal University, Ministry of Education, Changchun 130103, China

Деривати пиридина имају изражену способност координације, флексибилне електронске и оптичке особине, као и значајну стабилност као лиганди. Њихова супституциона модификација и проширена конјугација пружају идеалну платформу за изградњу ефикасних флуоресцентних сонди, катализатора и биолошки функционалних материјала. Имајући то у виду, синтетисан је нови $[Zn(phen)(L)(H_2O)]\cdot 4H_2O$ комплекс у солвотермалним условима, користећи 1,10-фенантролин (phen), 3-карбокси-1-карбоксиметил-2-оксидопиридинијум (H_2L) и Zn(II). Кристална структура и састав координационог једињења потврђени су методом дифракције X-зрака са монокристала и термогравиметријском анализом. Структурна анализа синтетисаног једињења је потврдила његову јединствену координациону геометрију. Поред тога, једињење испољава значајну луминисценцију, што га чини кандидатом за примену у сензорима. Луминисцентне и сензорске особине синтетисаног координационог једињења детаљно су испитиване. Нађено је да вредности K_{sv} константе за детекцију Fe^{3+} и ацетилацетона (acac) износе $3{,}29\times10^5$ M^{-1} и $6{,}67\times10^5$ M^{-1}, што потврђује високу и ефикасну способност детекције синтетисаног сензора.

(Примљено 2. јуна, ревидирано 1. јула, прихваћено 15. септембра 2025)

REFERENCES

1. M. S. Wang, X. T. Liu, B. C. Pan, S. J. Zhang, *Chemosphere* **93** (2013) 2877 (https://doi.org/10.1016/j.chemosphere.2013.08.082)
2. S. Yao, H. Xu, T. Zheng, Y. Li, H. Huang, J. Wang, J. Chen, S. Liu, H. Wen, *Chin. Chem. Lett*. **34.4** (2023) 107532 https://doi.org/10.1016/j.cclet.2022.05.046
3. Y. N. Wang, H. Xu, S. D. Wang, R. Y. Mao, L. M. Wen, S. Y. Wang, L. J. Liu, Y. Sun, S. Q. Liu, F. Wang, Q. F. Yang, *Spectrochim. Acta, A* **286** (2023) 121952 (https://doi.org/10.1016/j.saa.2022.121952)
4. X. Zhang, X. Zhuang, N. Zhang, C. Ge, X. Luo, J. Li, J. Wu, Q. Yang, R. Liu, *CrystEngComm* **21** (2019) 1948 (https://doi.org/10.1039/c9ce00068b)
5. W. Liu, H. Cui, J. Zhou, X. Chen, H. Yang, J. Wang, *J. Mol. Struct.* **1302** (2024) 137468 (https://doi.org/10.1016/j.molstruc.2023.137468)
6. L. L. Liu, H. W. Zhang, J. Y. Ren, L. Wang, Y. Zhang, *Spectrochim. Acta, A* **331** (2025) 125762 (https://doi.org/10.1016/j.saa.2025.125762)
7. Z. ul Nisa, M. Ahmad, H. N. Sheikh, *New J. Chem*. **48** (2024) 3100 (https://doi.org/10.1039/D3NJ05433K)
8. B. Zhao, J. Lu, H. Liu, S. Li, Q. Sun, B. Zhang, *CrystEngComm* **26** (2024) 1319 (https://doi.org/10.1039/D3CE01174G)
9. Á. González-Domínguez, F. M. Visiedo-García, J. Domínguez-Riscart, R. González--Domínguez, R. M. Mateos, A. M. Lechuga-Sancho, *Int. J. Mol. Sci*. **21** (2020) 5529 (https://doi.org/10.3390/ijms21155529)

10. J. B. Araškov, A. Višnjevac, J. Popović, V. Blagojević, H. S. Fernandes, S. F. Sousa, I. Novaković, J. M. Padrón, B. B. Holló, M. Monge, M. Rodríguez-Castill, *CrystEngComm* **24.29** (2022) 5194 (https://doi.org/10.1039/D2CE00443G)
11. C. Bizzarri, E. Spuling, D. M. Knoll, D. Volz, S. Bräse, *Coord. Chem. Rev*. **373** (2018) 49 (https://doi.org/10.1016/j.ccr.2017.09.011)
12. P. Ristić, T. R. Todorovic, V. Blagojević, O. R. Klisuric, I. Marjanovic, B. B. Holló, P. Vulic, M. Gulea, M. Donnard, M. Monge, M. Rodríguez-Castillo, *Cryst. Growth Des.* **20** (2020) 4461 (https://doi.org/10.1021/acs.cgd.0c00287)
13. R. A. Khan, A. AlFawaz, I. Hasan, N. A. AlMuryyi, A. A. Alhamed, S. Laeeq, A. Alsalme, *New J. Chem*. **48** (2024) 1287 (https://doi.org/10.1039/D3NJ04709A)
14. J. Suebphanpho, J. Boonmak, *RSC Adv.* **14** (2024) 9781 (https://doi.org/10.1039/D4RA00500G)
15. G.M. Otero-Fuentes, V. Sánchez-Mendieta, A. Sánchez-Ruiz, R. A. Morales-Luckie, D. Martínez-Otero, J. Jaramillo-García, A. Dorazco-González, *J. Fluoresc.* **35** (2024) 3449 (https://doi.org/10.1007/s10895-024-03754-1)
16. K. X. Ma, Y. Y. Yuan, Y. T. Ren, Y. Yang, H. G. Hao, J. Lu, S. N. Wang, *ACS Appl. Nano Mater.* **7** (2024) 19448 (https://doi.org/10.1021/acsanm.4c03335)
17. M. T. Seuffert, A. E. Sedykh, T. C. Schäfer, J. Becker, K. Müller-Buschbaum, *Dalton Trans.* **54** (2025) 5075 (https://doi.org/10.1039/D4DT03149K)
18. M. C. Burla, R. Caliandro, B. Carrozzini, G. L. Cascarano, C. Cuocci, C. Giacovazzo, G. Polidori, *J. Appl. Crystallogr.* **48** (2025) 306 (https://doi.org/10.1107/S1600576715001132)
19. G. M. Sheldrick, *Cryst. Struct. Chem.* **71** (2015) 3 (https://dx.doi.org/10.1107/S2053229614024218)
20. W. Liu, H. Cui, J. Zhou, X. Chen, H. Yang, J. Wang, *J. Mol. Struct*. **1302** (2024) 137468 (https://doi.org/10.1016/j.molstruc.2023.137468)
21. H. Wang, S. Li, H. Zhang, B. Su, X. Wang, *Main Group Met. Chem*. **48** (2025) 20240029 (https://doi.org/10.1515/mgmc-2024-0029)
22. X. Li, Y. Huang, B. Liu, X. Wang, *Main Group Met. Chem.* **48** (2025) 20240013 (https://doi.org/10.1515/mgmc-2024-0013)
23. Y. Hanifehpour, B. Mirtamizdoust, J. Dadashi, R. Wang, M. Rezaei, M. Abdolmaleki, S. W. Joo, *Crystals* **12** (2022) 113 (https://doi.org/10.3390/cryst12010113)
24. L. Gao, C. Jiao, H. Chai, Y. Ren, G. Zhang, H. Yu, L. Tang, 284 (2020) 121199, *J. Solid State Chem*. **284** (2020) 121199 (https://doi.org/10.1016/j.jssc.2020.121199).